Mass-based readout for agglutination assays

Rumi Chunara
Harvard-MIT Division of Health Sciences and Technology, Cambridge, Massachusetts 02139, USA

Michel Godin and Scott M. Knudsen
Biological Engineering Department, Massachusetts Institute of Technology, Cambridge, Massachusetts 02139, USA

Scott R. Manalis[a)]
Biological Engineering and Mechanical Engineering Departments, Massachusetts Institute of Technology, Cambridge, Massachusetts 02139, USA

(Received 21 September 2007; accepted 17 October 2007; published online 6 November 2007)

We present a mass-based readout for agglutination assays. The suspended microchannel resonator (SMR) is used to classify monomers and dimers that are formed during early stage aggregation, and to relate the total count to the analyte concentration. Using a model system of streptavidin functionalized microspheres and biotinylated antibody as the analyte, we obtain a dose-response curve over a concentration range of 0.63–630 nM and show that the results are comparable to what has been previously achieved by image analysis and conventional flow cytometry. © *2007 American Institute of Physics*. [DOI: 10.1063/1.2806197]

Agglutination assays based on nanometer and micrometer sized particles were originally inspired by natural agglutination of cells[1] and provide a simple and rapid means for diagnostic testing. There are several commercial examples[2] of agglutination assays used for clinical diagnostics applications. These assays are typically straightforward to administer and provide fast response times.[3] Techniques for measuring agglutination include turbidimetry,[4] dynamic light scattering,[5] and UV-vis spectroscopy.[6] In some cases, particle counting techniques such as flow cytometry and image analysis can improve sensitivity by quantifying small aggregates that are produced during the initial stages of aggregation,[7] allowing for a reduction of the required incubation times. Additionally, particle counting enables more specific information about the agglutination distribution in a population, rather than average agglutination information typically obtained by ensemble measurement techniques. Furthermore, microfluidic approaches for particle counting can reduce the required sample volume from milliliters to microliters and enable integration with sample treatment steps.[8]

In this letter, we present a non-optical alternative for particle counting where early stage aggregation is quantified by measuring mass with the suspended microchannel resonator (SMR). In SMR detection,[9] each aggregate is weighed in real time by measuring transient changes in resonant frequency as it flows through the vibrating microchannel (Fig. 1). Using a model system of streptavidin functionalized microspheres and biotinylated antibody as the analyte [Fig. 1(a)], we obtain a dose-response curve showing particle agglutination over a concentration range of 0.63–630 nM. We show that the results are comparable to what has been previously achieved by image analysis and conventional flow cytometry.[7]

The biotin-streptavidin model system enabled us to take advantage of the high binding affinity reaction, as well as to make comparison to previously demonstrated detection techniques[7] for agglutination. We chose 0.97 μm spherical streptavidin-labeled polystyrene microspheres to enable visualization by optical microscopy. The analyte consisted of anti-FLAG M5 monoclonal antibody biotinylated with approximately six biotins per antibody (Sigma Aldrich, St. Louis, MO). The microspheres were centrifuged, washed,

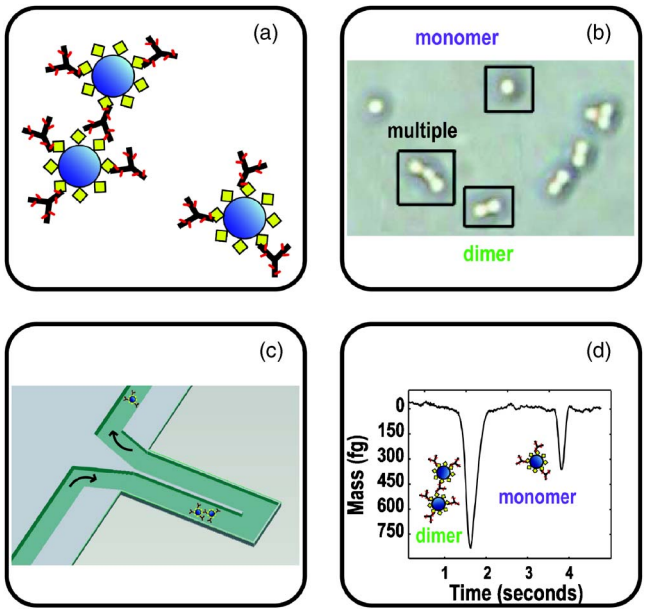

FIG. 1. (Color online) (a) Streptavidin (SA)-coated microspheres are incubated with the target protein (SA is illustrated by diamonds). The analyte (biotinylated antibody) creates agglutination by binding to two different SA receptors located on separate microspheres. (b) Optical micrograph of monomer, dimer, and multimer structures which are formed by agglutination of 0.97 μm SA microspheres with 0.63 nM of analyte. (c) Schematic of the suspended microchannel resonator (SMR) for counting aggregates by weighing them one at a time. The resonance frequency of the SMR is sensitive to the presence of particles whose mass density differs from that of the solution in the microfluidic channel. (d) The SMR is used to classify a monomer (right) and a dimer (left) and anything larger as a multimer (not shown). The transient frequency shift from each structure is converted to a mass by using a calibration factor (see Ref. 9) and accounting for the buffer density.

[a)]Electronic mail: scottm@media.mit.edu

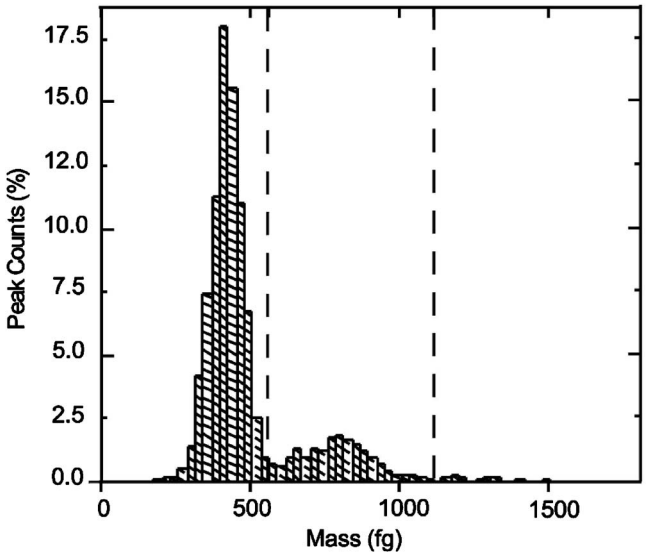

FIG. 2. Mass histogram from aggregates weighed by the SMR. There are primarily two types of structures (monomers and dimers) that resulted from an analyte concentration of 6.3 nM and a particle concentration of 5×10^8 particles/ml. In each experiment approximately 2000 peaks were counted in 2 h. Particle types were classified by integrating the number of agglomerates between 0 and 566 fg for monomers, 566 and 1132 fg for dimers, and 1132 fg and above for multimers (thresholds marked by dashed lines).

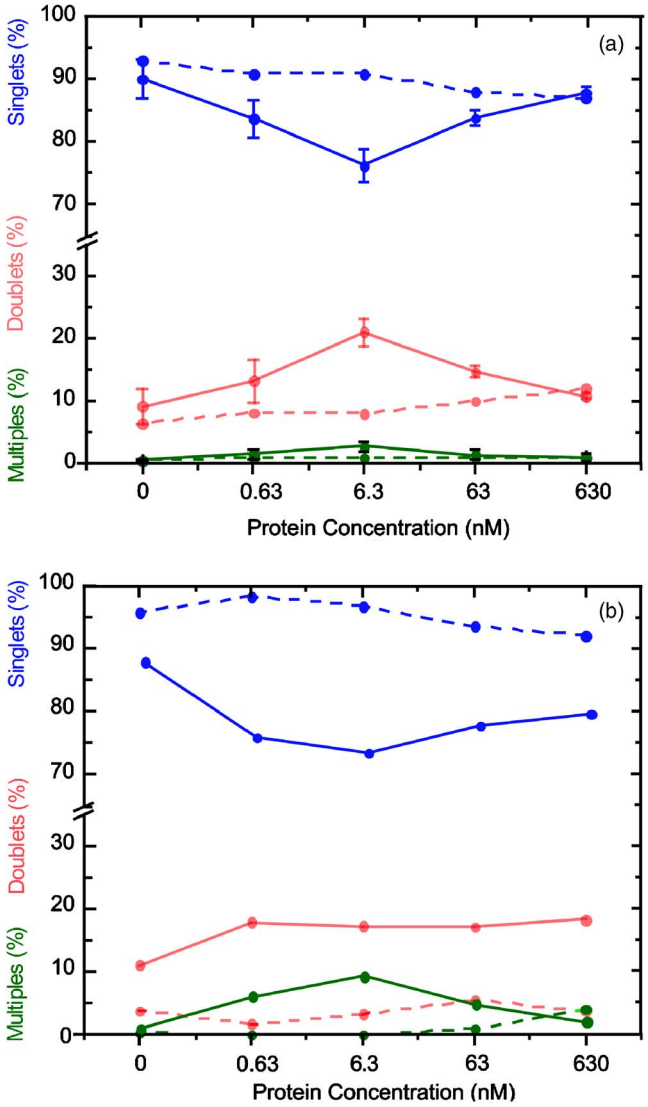

FIG. 3. (Color online) (a) Mass-based dose response curve obtained by weighing aggregates with the SMR. Each data point represents the mean obtained from three experiments, and at 0.63 nM, five experiments. The dependence of structure proportion is shown vs analyte concentration (biotinylated antibody in solid lines and pure antibody in dashed lines). Each data point represents the mean percentage of structures obtained from three separate experiments at each concentration. In each experiment approximately 2000 aggregates were weighed, and error bars represent the standard deviation from the mean. (b) A dose response curve was also obtained by optically imaging approximately 1500 aggregates per analyte concentration.

and resuspended in buffer [phosphate-buffered saline (PBS), pH 7.2 with 0.1% bovine serum albumin and 1% Tween 20] at a concentration of 2×10^{10} particles/ml. To minimize nonspecific aggregation, the microspheres were then ultrasonicated for 3 min (15 s on, 10 s off). The biotinylated antibody analyte was added to give final concentrations of 0, 0.63, 6.3, 63, and 630 nM, and the mixtures were incubated for 30 min at 25 °C with gentle mixing at 15 and 25 min. After incubation, the sample was diluted with PBS to quench the reaction and create a final particle concentration of approximately 5×10^8 particles/ml, which has previously been determined to optimize throughput while decreasing the probability that two or more aggregates simultaneously pass through the SMR channel.[9]

Due to the short incubation time, we were able to observe the early stages of the agglutination reaction when the solutions consisted mostly of monomer and dimer structures, with any larger structures grouped as "multimers." For visualization by optical microscopy, solutions were prepared as above and left for 10 min on glass slides before viewing to allow structures to settle into a single layer and be counted [Fig. 1(b)]. For detection with the SMR, we classified structures by flowing the solution through the device and weighing aggregates one by one [Fig. 1(d)].

In order to obtain a dose-response curve using the SMR, a mass histogram from approximately 2000 aggregates was acquired at each analyte concentration. As an example, Fig. 2 shows the mass histogram for an analyte concentration of 6.3 nM. Here, two clearly distinguishable distributions reveal the monomer and dimer proportions in the sample. The relative area under each of these distributions changes as the analyte concentration is varied. The monomer and dimer distributions of Fig. 2 overlap due to the polydispersity of the polystyrene particles (5%–10%),[10] which contributes to some uncertainty in the measured aggregate fraction. Moreover, differently sized particles within the nominal distribution may have different binding capacities which could also contribute to uncertainty. For consistency, a value of 566 fg was chosen as the threshold between monomer and dimer populations for all experiments, and all peaks above 1132 fg were classified as multimers.

The percentage of each structure is plotted versus analyte concentration in the dose response curve shown in Fig. 3(a). In order to confirm the trend of the dose response curve, optical microscopy was used to classify approximately 1500 structures that were agglutinated at each of the same analyte concentrations as measured by the SMR [Fig. 3(b)]. For optical and SMR based readout, the proportion of dimers and multiples in the sample increases as the analyte protein concentration is increased from zero up to 6.3 nM. Beyond this concentration, the number of dimers and multiples decreases as the number of monomers in-

creases due to saturation of the particles by the biotinylated antibody. This hook effect,[11] whereby the slope of the dose response curve changes sign past the "equivalence point," is visible after the data point at 6.3 nM. Negative control experiments (antibody without biotin) do not demonstrate this phenomenon (Fig. 3).

As outlined by Wiklund *et al.*,[7] the detection limit of an agglutination assay scales linearly with the particle concentration and binding capacity provided that the capacity is greater than the binding affinity constant. The dynamic range of agglutination assays is typically limited to the range between the minimum detectable concentration and the equivalence point. For the data shown in Fig. 3(a), the dynamic range is approximately tenfold, which is comparable to what was achieved by optical inspection [Fig. 3(b)], and in prior work, by flow cytometry and image analysis.[7] While the optical and SMR dose response curves in Fig. 3 show similar trends for monomers, a relatively larger percentage of multimer aggregates are measured optically. This is likely attributed to larger structures either not flowing into the suspended microchannel due to size constraints (the fluidic channel inside the cantilever is 3 μm tall by 8 μm wide), structures breaking because of shear forces in the microchannel, or settling of the larger aggregates. The SMR's tendency to undercount aggregates of three or more particles could be reduced by using smaller particles.

Limited sample size (total number of aggregates counted in an experiment) may contribute to uncertainty in the proportions of structures at each analyte concentration. However, the sample size along with the particle counting rate determines the total measurement time for each assay. In order to determine the extent to which sample size contributes to overall error between experiments, the standard deviation from three experiments was calculated over a range of sample sizes. At the analyte concentration of 0.63 nM, the mean proportion of monomers was calculated by using the first 1000 counts, the first 1500, and up to a sample size of 3500. The resulting standard deviation is plotted in Fig. 4 and is normalized to the standard deviation from 2000 counts in order to enable a comparison to error bars shown in Fig. 3(a). The standard deviation continues to decrease with sample sizes larger than 2000 which implies that the uncertainty in Fig. 3 could be reduced still by measuring more aggregates.

In conclusion, our results demonstrate mass readout with the SMR as a method for classification of analyte-induced particle agglutination. We use the SMR to enumerate monomers and dimers associated with the early stages of particle agglutination. The sensitivity and dynamic range achieved in this work is considerably less than what can be achieved with a surface-based assay inside the SMR.[9] However, SMR agglutination assays do not require functionalization of the SMR channel walls, and assays can be developed and prepared independently of the device. Furthermore, particles with a wide range of functionalities and sizes are readily available, enabling assays with varying reaction rates and aggregate sizes. Moreover, multiple analytes may be detected simultaneously within the same mixture by multiplexing particles with differing masses. In terms of readout, the SMR has an equivalent noise level of 1 fg (1 Hz bandwidth),

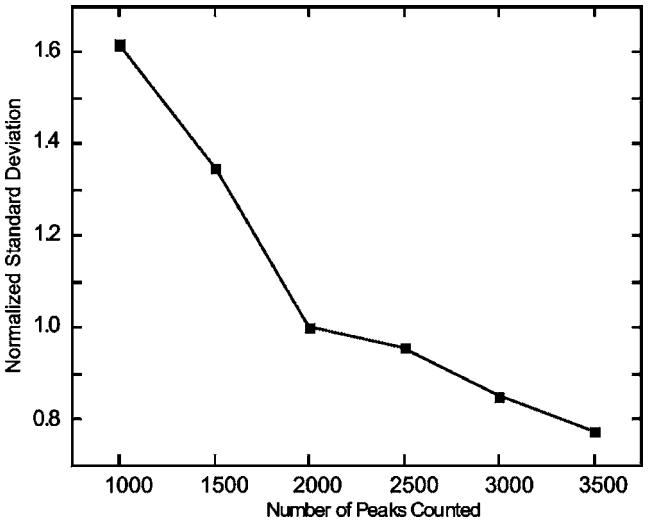

FIG. 4. Normalized standard deviation (SD) of the mean percentage of monomers versus the number of aggregates counted (normalized to the SD at 2000 counts). Aggregates were counted for 4 h in each of three experiments using the same concentration analyte (0.63 nM biotinylated protein). The data point at 2000 counts includes data from two earlier experiments, representing five experiments total. The number of monomers was examined for the first 1000 counts and up to 3500 counts in increments of 500.

which enables structures equivalent to 100 nm gold, 300 nm silica, or 700 nm polystyrene particles to be detected in water with a signal-to-noise ratio of 10. Reduction in device size will ultimately enable the measurement of even smaller particles. In order to achieve the current resolution, the counting rate is limited to approximately 1 particle/s, which is considerably slower than traditional optical approaches. However, the SMR is amenable to parallel detection and integration with microfluidic systems, and work to fabricate suspended microchannel arrays with integrated piezoresistive sensors is currently underway.

We thank Geoffrey von Maltzahn, Amit Agrawal, and Ken Babcock for valuable discussions and acknowledge financial support from the National Institutes of Health (NIH) Cell Decision Process Center Grant and the Institute for Collaborative Biotechnologies from the U.S. Army Research Office. M.G. acknowledges support from the Natural Sciences and Engineering Research Council of Canada (NSERC) through a postdoctoral fellowship.

[1]C. M. Plotz and J. M. Singer, Am. J. Med. **21**, 888 (1956).
[2]Rapid Diagnostic Tests (http://www.rapid-diagnostics.org/) Trinity Biotech (http://www.trinitybiotech.com/) Wako USA (http://www.wakousa.com/).
[3]S. Eda, J. Kaufmann, W. Roos, and S. Pohl, J. Clin. Lab Anal **12**, 137 (1998).
[4]O. Deegan, K. Walshe, K. Kavanagh, and S. Doyle, Anal. Biochem. **312**, 175 (2003).
[5]T. Antony, A. Saxena, K. B. Roy, and H. B. Bohidar, J. Biochem. Biophys. Methods **36**, 75 (1998).
[6]S. Narayanan, S. Orton, G. F. Leparc, L. H. Garcia-Rubio, and R. L. Potter, Transfusion (Bethesda, Md.) **39**, 1051 (1999).
[7]M. Wiklund, O. Nord, R. Gothall, A. V. Chernyshev, P. A. Nygren, and H. M. Hertz, Anal. Biochem. **338**, 90 (2005).
[8]N. Pamme, R. Koyama, and A. Manz, Lab Chip **3**, 187 (2003).
[9]T. P. Burg, M. Godin, S. M. Knudsen, W. Shen, G. Carlson, J. S. Foster, K. Babcock, and S. R. Manalis, Nature (London) **446**, 1066 (2007).
[10]Bangs Laboratories.
[11]S. A. Fernando and G. S. Wilson, J. Immunol. Methods **151**, 47 (1992).